IET Science, Measurement & Technology

Research Article

# Altitude data fusion utilising differential measurement and complementary filter

ISSN 1751-8822
Received on 25th March 2016
Revised on 22nd June 2016
Accepted on 18th July 2016
doi: 10.1049/iet-smt.2016.0118
www.ietdl.org

*Sheng Wei, Gu Dan* ✉*, Hu Chen*

*School of Instrumental Science and Optical Electronics Engineering, BeiHang University, No. 39 Xueyuan Road, Beijing, People's Republic of China*

✉ *E-mail: gudan@buaa.edu.cn*

**Abstract:** In plenty of researches and real systems, barometer and accelerometer which can provide altitude and acceleration measurements, respectively, are utilised in altitude estimation of small unmanned aerial vehicle. These sensors can draw on their merits and improve the accuracy of altitude estimation. The altitude measurement of barometer has the drift problem as one of its disadvantages which could deteriorate the performance of altitude estimation. In addition, barometer and accelerometer both have stochastic error which reduce the accuracy of altitude estimation. A novel scenario is proposed by utilising differential altitude measurement and complementary filter to deal with above issues. It is accurate and suitable for real-time application. In this scenario, altitude drift is reduced by using differential altitude measurement, and the stochastic error of altitude is minimised by using complementary filter algorithm. Stair and flight experiments are implemented to test this scenario. The experimental results indicate that it can provide good dynamic performance and flexibility for altitude estimation.

## 1 Introduction

To utilise the best performance of each sensor, multi-information fusion technique has been widely used in unmanned aerial vehicle (UAV) system. The altitude-measuring sensors include barometer, global navigation satellite system (GNSS) receiver, laser ranging sensor, sonar sensor, camera sensor and so on. Small unmanned aerial vehicle (SUAV) is equipped with inertial navigation system (INS), GNSS receiver, barometer, airspeed meter, magnetic compass and other sensors [1, 2]. In order to obtain the altitude estimation and vertical velocity of the vehicle, barometer, GNSS receiver, and accelerometer are widely used. Barometer provides altitude of vehicle, but it cannot get the vertical velocity. Furthermore, pressure altitude has the problems of drift and delay that are more severe in low-cost sensors. GNSS receiver provides three-dimensional position information, velocity information and time information. The error of GNSS does not accumulate over time, but the performance of altitude is less accurate than horizontal position's performance. The output frequency of GNSS is relatively low. Besides, GNSS provides reliable position velocity time on condition that at least four satellites are visible in open sky outdoor environment [3]. Accelerometer can provide the acceleration of SUAV with sensitivity and high update rate. However, it has drift error that will result in divergence of position and velocity estimation [4]. Since every sensor has advantages and limits, how to make these sensors complementary to achieve better performance is still a hot topic in academic researches.

In the area of altitude estimation, Kalman filter is used to fuse altitude of barometer and acceleration in some literatures [5, 6]. Altitude estimated result with Kalman filter has drift error in [6], and the pressure sensor used in this work and our work is the same. In our work, to cope with the drift error of low-cost pressure sensor, we use differential altitude measurement. An altitude fusion method which uses consistency fusion and BP neural network is proposed in [7]. This method has higher precision, but longer fusion time than consistency. A robust location estimation algorithm by fusing data from barometric altimeter and topographic map is presented in [8], and other method as using vision technology to estimate altitude is described in [9, 10]. In many researches [11–14], complementary filter is utilised to estimate motions and attitudes because of the complementary characteristic of accelerometers and gyroscopes. In our work, complementary filter is used for altitude data fusion particularly. Pressure sensor and ultrasonic sensor are used for altitude estimation for UAV application in [1], and low-pass filter is for minimising the influence of noise pressure sensor. We utilise complementary filter which fuse both pressure altitude and acceleration information to estimate altitude in our work. Because of the good dynamic characteristic of acceleration, altitude estimation by complementary filter performs better as for dynamic condition and precision. Compared with Kalman filter, complementary filter is more efficient as for computational complexity.

Considering low-cost and real-time application, pressure altitude and acceleration are used to estimate altitude by complementary filter algorithm in this paper. Base barometer and rover barometer are used to produce differential altitude measurement to reduce the drift caused by changes of atmospheric environment. Altitude estimation can also be obtained by inertial INS. The algorithm to estimate altitude by pure INS is integral algorithm, and the error of altitude estimation is accumulated over time [15]. The error of barometer is not divergent. Hence it is essential to use both barometer and inertial measurement units (IMU) to estimate altitude. Because of the complementary property of barometer and accelerometer, complementary filter outperforms in reducing random error of altitude estimation. The main contribution of this paper is introduction and experiments of the novel scenario by utilising differential altitude measurement and complementary filter to obtain altitude estimation. The rest of this paper is structured as follows. The sensors used in data fusion system are described in Section 2. Efficiency of differential altitude measurement is described in Section 3. Complementary filter for altitude estimation and designing for the altitude data fusion scenario are presented in Section 4. Experimental result is presented in Section 5. Finally, the conclusions are drawn in Section 6.

## 2 Sensors used in altitude data fusion

This section is focused on making a brief introduction to the sensors used in altitude data fusion system. Barometer and IMU are the main members of the system in terms of low-cost and real-time

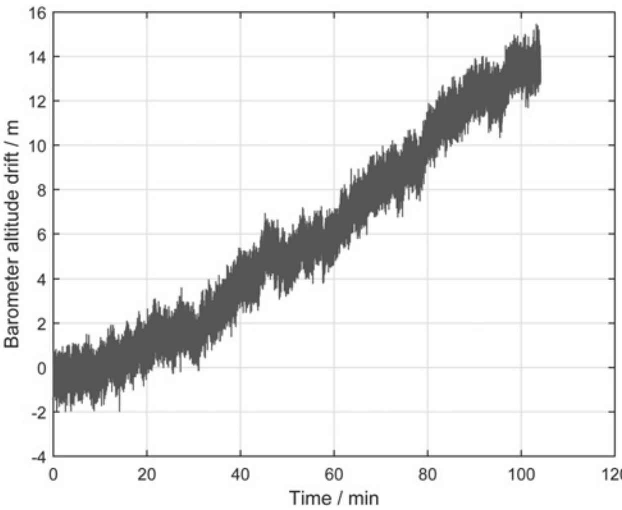


**Fig. 1** *Drift error of altitude calculated by barometer*

application. IMU is composed of gyroscopes and accelerometers. In this study, micro-electromechanical systems (MEMS) IMU is used because of smaller size, lighter weight and lower price [6].

### *2.1 Barometer*

As given in (1), the atmospheric pressure can be computed at a corresponding altitude and temperature [1]. The coefficients are defined as follows. Where $P_H$ is atmospheric pressure at the altitude of $H$. $P_b$ is atmospheric pressure at the altitude of $H_b$. $T_b$ is temperature, and $\beta$ is temperature lapse rate ($\beta = -6.5 \times 10^{-3}$ K/m under 11 Km). $g_0$ is Earth-surface gravitational acceleration. $R$ is universal gas constant ($R = 287.05287 J/(K \cdot kg)$).

$$P_H = P_b\left[1 + \frac{\beta}{T_b}(H - H_b)\right]^{(-g_0/\beta R)} \tag{1}$$

From the above equation, the absolute altitude can be derived as follows.

$$H = \frac{T_b}{\beta}\left[\left(\frac{P_H}{P_b}\right)^{(-\beta R/g_0)} - 1\right] + H_b \tag{2}$$

Besides atmospheric pressure, we also need temperature to compute altitude. In this work, we use BMP085 digital pressure sensor as pressure sensor, and it can provide both pressure measurement and accurate temperature measurement. In real application, altitude can be computed by linear model which can decrease the computing load. In order to use linear model to compute altitude, temperature calibration is pretty essential. In linear model, a pressure change of $\Delta p = 1 hpa$ corresponds to 8.43 m at sea level. The altitude computed by the barometer is presented in Fig. 1, and the test platform is still during the experiment. The raw pressure data output from barometer are collected for more than 1 h. There are still two main types of errors existing after temperature compensation. The first error is drift error caused by changes of atmospheric environment and disturbances in pressure [16]. The second error is stochastic error. These errors have negative effect on estimation of altitude. To this point, a novel data fusion scenario is developed by using differential altitude measurement and complementary filter to reduce these errors. Differential altitude measurement can diminish the former error, while complementary filter can diminish the latter error. The detail of differential altitude measurement and complementary filter will be introduced in Sections 3 and 4, respectively.

### *2.2 Accelerometer*

The acceleration fused by complementary filter is $a_U$ in navigation frame, but the acceleration collected from accelerometers $(a_x^b, a_y^b, a_z^b)$ is in body frame. The navigation frame is defined as E-N-U (East, North, Upward) coordinate in this paper. It is essential to compute transformation matrix $\boldsymbol{C}_b^n$ in order to obtain $a_U$. The process of computing $a_U$ is presented in Fig. 2. IMU system can provide both angular rate and acceleration in body frame. First, quaternion updating algorithm is used for computing $\boldsymbol{q}$ and attitude angle $(\theta, \phi, \psi)$. Then transformation matrix can be computed either by $(\theta, \phi, \psi)$ or quaternion $q$. In this work, $\boldsymbol{C}_b^n$ is computed by $(\theta, \phi, \psi)$. Finally, $a_U$ is worked out by coordinate transform. $(\theta, \phi, \psi)$ updated by $q$ is presented in (3). Transformation matrix $\boldsymbol{C}_b^n$ is presented in (4), while $a_U$ can be computed by $\boldsymbol{C}_b^n$ as (5).

$$\begin{cases} \phi = a\tan\left(\dfrac{2(q_0q_2 - q_1q_3)}{1 - 2(q_1^2 + q_2^2)}\right) \\ \theta = a\sin(2(q_2q_3 + q_0q_1)) \\ \psi = a\tan\left(\dfrac{2(q_1q_2 - q_0q_3)}{1 - 2(q_1^2 + q_3^2)}\right) \end{cases} \tag{3}$$

(see (4))

$$(a_E, a_N, a_U)^{\mathrm{T}} = \boldsymbol{C}_b^n \cdot (a_x^b, a_y^b, a_z^b)^{\mathrm{T}} \tag{5}$$

Actually accelerometer is sensitive to vibration, hence the accelerometers equipped on the UAV is influenced by vibratory noise inevitably during flight. So it is necessary to use filter to reduce the vibratory noise. In this work, low-pass filter algorithm is used, and the equations are as follows. In (6), $a_k$ is raw acceleration. $b_j$ is weighting factor. $x_k$ is intermediate variable, and $y_k$ is output of the filter.

$$\begin{aligned} x_k &= \frac{1}{3}\sum_{i=0}^{2} a_{k-i} \\ y_k &= \frac{1}{5}\sum_{j=0}^{4} b_j \cdot x_{k-j} \end{aligned} \tag{6}$$

## 3 Efficiency of the differential altitude measurement

As shown in Fig. 1, there is drift error in pressure altitude which is caused by changes of atmospheric environment and disturbances. Considering the drift error, two barometers can be used to produce differential altitude measurement to overcome the issue. One of the barometers named base barometer keeps still on the ground, while the other named rover barometer is mounted on the UAV. During the close flight of UAV, if differential altitude measurement is utilised for altitude estimation, drift error can be decreased effectively. The base platform and rover platform are equipped with the same barometers. Differential altitude measurement can restrain the common drift error caused by changes of atmospheric environment between base barometer and

$$\boldsymbol{C}_b^n = \begin{bmatrix} \sin\phi\sin\theta\sin\psi + \cos\phi\cos\psi & \cos\theta\sin\psi & \sin\phi\cos\psi - \cos\phi\sin\theta\sin\psi \\ \sin\phi\sin\theta\cos\psi - \cos\phi\sin\psi & \cos\theta\cos\psi & -\cos\phi\sin\theta\cos\psi - \sin\phi\sin\psi \\ 3pt - \sin\phi\cos\theta & \sin\theta & \cos\phi\cos\theta \end{bmatrix} \tag{4}$$

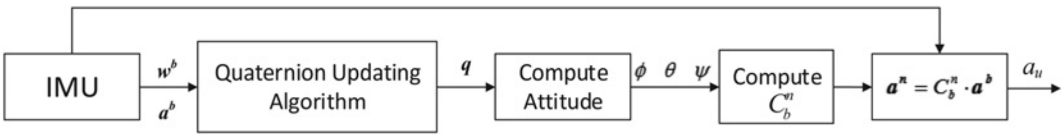


**Fig. 2** *Process of computing $a_U$*

**Table 1** Variable definition of differential altitude model

| | |
|---|---|
| $H_{\mathrm{pb}}$: pressure altitude of base platform | $H_{\mathrm{b}}$: true altitude of base platform |
| $h_{\mathrm{fb}}$: drift of base pressure altitude | $r_{\mathrm{b}}$: random error of base pressure altitude |
| $H_{\mathrm{pr}}$: pressure altitude of rover platform | $H_{\mathrm{r}}$: true altitude of rover platform |
| $h_{\mathrm{fr}}$: drift of rover pressure altitude | $r_{\mathrm{r}}$: random error of rover pressure altitude |

rover barometer as (7). The variable is defined as Table 1.

$$\begin{cases} H_{\mathrm{pb}} = H_{\mathrm{b}} + h_{\mathrm{fb}} + r_{\mathrm{b}} \\ H_{\mathrm{pr}} = H_{\mathrm{r}} + h_{\mathrm{fr}} + r_{\mathrm{r}} \\ H_{\mathrm{pdiff}} = H_{\mathrm{pr}} - H_{\mathrm{pb}} = H_{\mathrm{rb}} + (h_{\mathrm{fb}} - h_{\mathrm{fr}}) + (r_{\mathrm{b}} - r_{\mathrm{r}}) \\ H_{\mathrm{pdiff}} \simeq H_{\mathrm{rb}} + (r_{\mathrm{b}} - r_{\mathrm{r}}) \end{cases} \tag{7}$$

In the same atmospheric environment, $h_{\mathrm{fb}}$ is approximately equal to $h_{\mathrm{fr}}$. $H_{\mathrm{pdiff}}$ is differential altitude measurement between base pressure altitude and rover pressure altitude. $H_{\mathrm{rb}}$ is relative altitude between base platform and rover platform.

The efficiency of the differential altitude measurement is experimentally evaluated in stair tests. The base platform and rover platform are 30 m apart in Fig. 3. The platforms used in the experiment are shown in Fig. 4. The barometer data and accelerometer data are collected at a rate equal to 100 Hz. The base barometer is still during the whole experiment, and it is on the first floor. The rover barometer is on the first floor at the beginning of the experiment. Rover platform starts moving up at the moment of 40 min, illustrated in Fig. 3. The rover platform moves up from first floor to the sixth floor, and then it stands still for about 20 min. At last it moves back from the sixth floor to first floor. The rover platform keeps still for about 1 min in each floor. Each floor is approximately 4 m. It is evident that the drift of pressure altitude is more than 5 m in 1 h. Thanks to the differential altitude, the drift error is decreased significantly. Despite the differential pressure altitude is capable to reduce the drift error, the random error is greater. If the standard deviation $\sigma_0$ of the base altitude and rover altitude are considered to be same, the standard deviation of the differential altitude will increase to $\sqrt{2}\sigma_0$. To overcome this issue, complementary filter is adopted to minimise the random noise in this paper (Fig. 4).

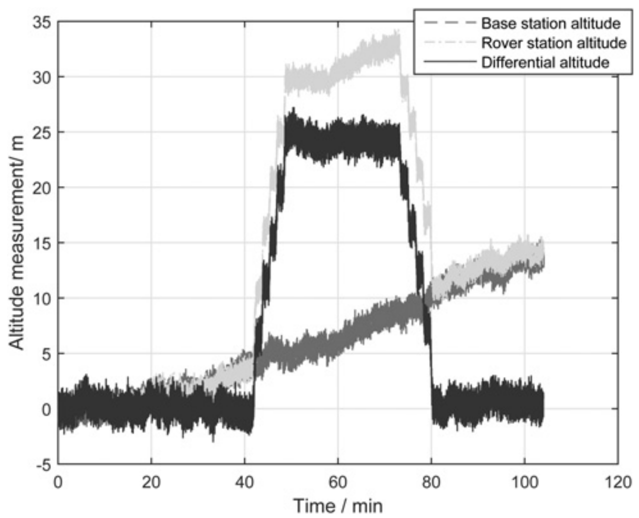


**Fig. 3** *Pressure altitude of base/rover platform and differential measurement*

## 4 Complementary filter

As shown in Fig. 1, besides drift error, there is a statistical error in pressure altitude. Moreover, the statistical error of the differential altitude measurement is greater. This issue becomes more demanding when differential altitude measurement is used for altitude estimation. Hence it is necessary to find an effective solution to solve this issue.

It is evident that the random error of pressure altitude is high-frequency random noise. In [1], low pass filter is used to improve the random noise. The altitude integrated by acceleration is divergent, and the statistical error of this altitude is low-frequency random noise [13]. Hence the statistical error of pressure altitude and the altitude integrated by acceleration is complementary in frequency domain. Thus complementary filter can be used to estimate altitude to achieve the best performance of pressure sensor and accelerometer. $a_u$ is the vertical acceleration calculated by accelerometers in navigation frame. $H_{\mathrm{baro}}$ is pressure altitude calculated by barometer. $\ddot{h}_a$ is the vertical acceleration. $h_b$ is the height, $\ddot{n}_1$ is the random noise of vertical acceleration calculated by accelerometers. $n_2$ is the random noise of pressure height calculated by barometer. $\hat{H}(s)$ is the estimation of the complementary filter.

$$a_u = \ddot{h}_a + \ddot{n}_1 \tag{8}$$

$$H_{\mathrm{baro}} = h_b + n_2 \tag{9}$$

$G_1(s)$ is second-order high-pass filter, and $G_2(s) = 1 - G_1(s)$ is

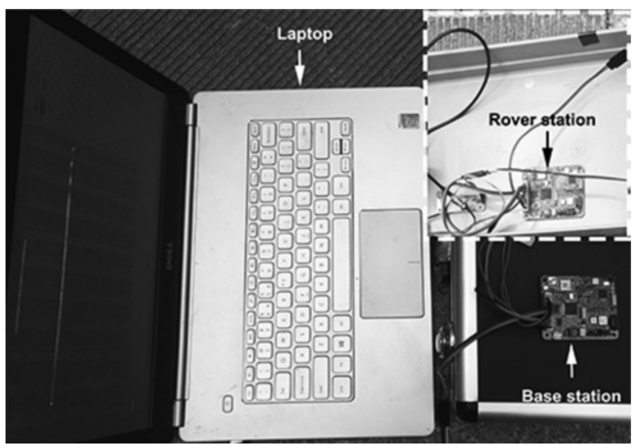


**Fig. 4** *Experimental system and equipment of rover platform and base platform*

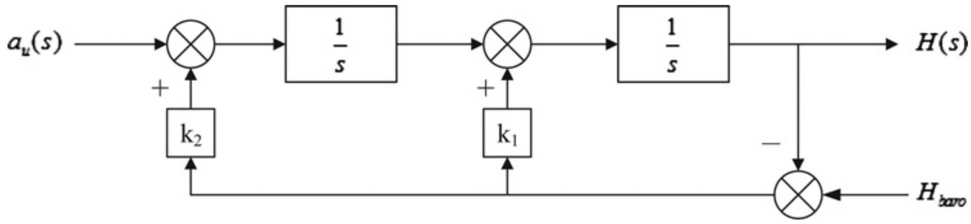


**Fig. 5** *Complementary filter mechanisation*

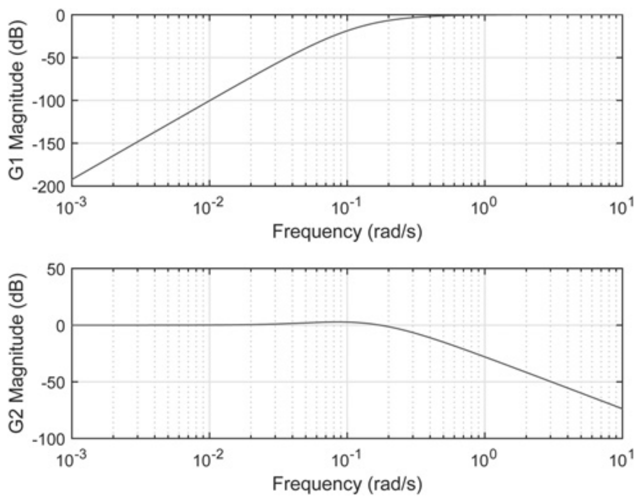


**Fig. 6** *Dynamic response of high-pass filter ($G_1$) and low-pass filter ($G_2$)*

low-pass filter. The transfer function of the filters are as follows.

$$G_1(s) = \frac{s^2}{s^2 + k_1 s + k_2} \tag{10}$$

$$G_2(s) = \frac{as + b}{s^2 + k_1 s + k_2} \tag{11}$$

Altitude measurement integrated by acceleration is filtered with high-pass filter, while differential altitude measurement calculated by barometer is filtered with low-pass filter. High-pass filter is capable of minimising the low-frequency random noise of the altitude integrated by acceleration, while the low-pass filter is capable of minimising the high-frequency random noise calculated by barometer. The equation of complementary filter applied in altitude estimation is derived as follows.

$$\hat{H}(s) = \frac{G_1(s)}{s^2}(\ddot{h}_a(s) + \ddot{n}_1(s)) + G_2(s)(h_b(s) + n_2(s)) \tag{12}$$

$$\hat{H}(s) = \frac{s^2}{s^2 + k_1 s + k_2}(h_a(s) + n_1(s)) + \frac{k_1 s + k_2}{s^2 + k_1 s + k_2}(h_b(s) + n_2(s)) \tag{13}$$

$$\hat{H}(s) = h(s) + \frac{s^2}{s^2 + k_1 s + k_2} n_1(s) + \frac{k_1 s + k_2}{s^2 + k_1 s + k_2} n_2(s) \tag{14}$$

$$\hat{H}(s) = \frac{1}{s^2}\left[\ddot{h}_a(s) + \ddot{n}_1(s) + k_2\left(h_b(s) - \hat{H}(s)\right)\right] + \frac{k_1}{s}\left(h_b(s) - \hat{H}(s)\right) \tag{15}$$

According to (15), the mechanisation of complementary filter is shown as Fig. 5 where $k_1$ and $k_2$ are feedback coefficients. The error signal is resulted from the difference of $\hat{H}(s)$ and $H_{\text{baro}}$, and then the error signal is fed back to the two integrity components. When $k_1 = 0.25$, $k_2 = 0.015$, dynamic responses of high-pass filter ($G_1$) and low-pass filter ($G_2$) are shown in Fig. 6.

In this work, the data fusion scenario utilising differential altitude measurement and complementary filter is presented in Fig. 7. The vertical acceleration in navigation frame can be calculated by IMU system. Then the vertical acceleration is passed into low-pass filter to decrease the vibration. Meanwhile, both the base and rover barometers' output should be compensated by temperature calibration first, and then comes the differential altitude calculated

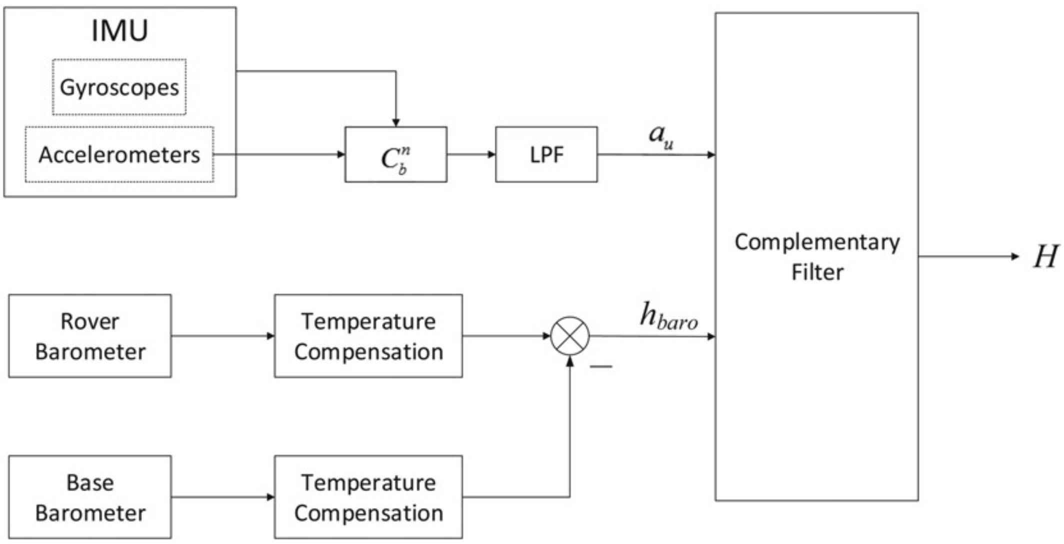


**Fig. 7** *Data fusion scenario utilising differential altitude measurement and complementary filter*

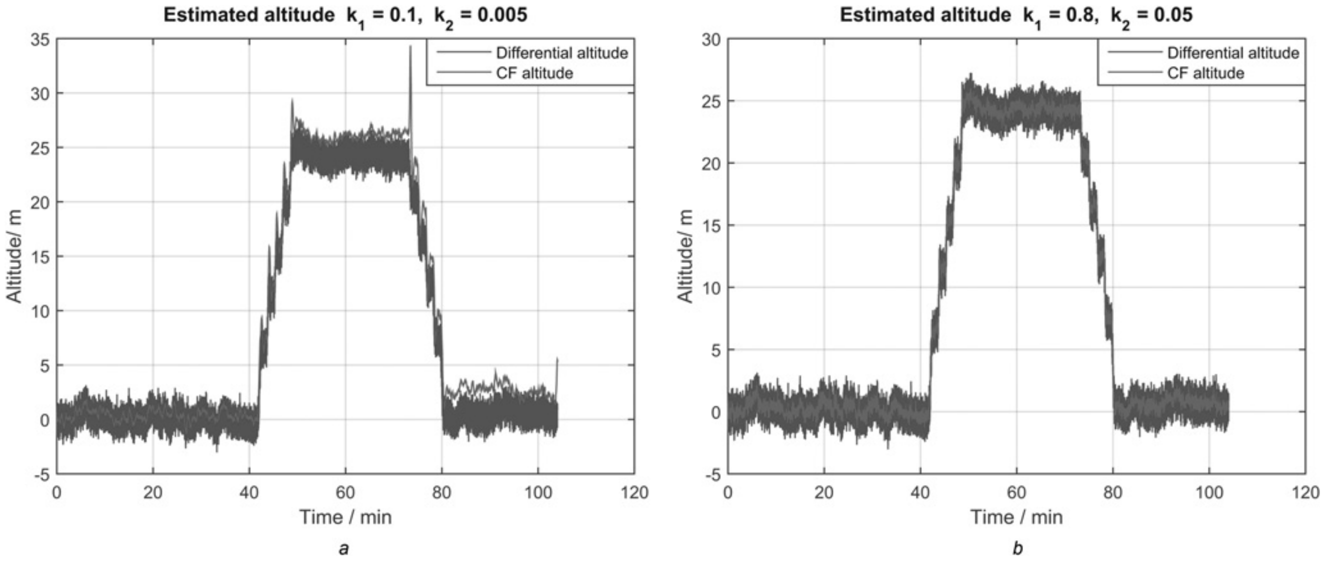


**Fig. 8** *Estimated altitude by using complementary filter and raw differential altitude measurement*
*a* Estimated altitude when $k_1 = 0.1$, $k_2 = 0.005$
*b* Estimated altitude when $k_1 = 0.8$, $k_2 = 0.05$

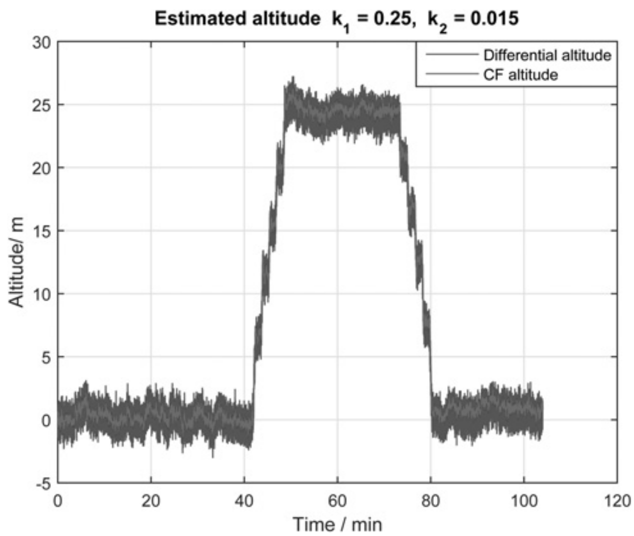


**Fig. 9** *Estimated altitude when $k_1 = 0.25$, $k_2 = 0.015$*

by base and rover barometers. The differential altitude and $a_u$ are passed into complementary filter to estimate altitude at last. Drift and random error can be decreased significantly by utilising differential altitude measurement and complementary filter.

## 5 Experimental result

To assess the performance of data fusion scenario for altitude estimation, stair tests and flight tests are designed by using low-cost sensors. The experiments are led as the scenario described in Section 4, hence differential altitude measurement and complementary filter were both used in the experiments.

**Table 2** Performance of estimated altitude

| $k_1$ | $k_2$ | STD, *m* | AVG, *m* |
|---|---|---|---|
| raw | raw | 0.4661 | 24.3027 |
| 0.1 | 0.005 | 0.0121 | 26.0775 |
| 0.8 | 0.05 | 0.1424 | 24.3271 |
| 0.25 | 0.015 | 0.0679 | 24.5616 |

The raw sensor data of Figs. 8 and 9 is the same as the experiment described in Section 3. $k_1$ and $k_2$ are given on the basis of noise characteristic of sensors and test. To analyse the result of experiment, complementary filter algorithm is run with different values of $k_1$ and $k_2$ (feedback coefficients) in Figs. 8 and 9. Fig. 8*a* illustrates the estimated altitude when $k_1 = 0.1$, $k_2 = 0.005$, and Fig. 8*b* illustrates the estimated altitude when $k_1 = 0.8$, $k_2 = 0.02$. While Fig. 9 illustrates the estimated altitude when $k_1 = 0.25$, $k_2 = 0.015$.

The performance of estimated altitude with respect to different coefficients is given in Table 2. STD is the standard deviation of altitude, while AVG is the mean value of estimated altitude. Raw is the raw pressure differential altitude. To make a contrast with raw measurement, the differential altitude is given in first line. When $k_1 = 0.1$, $k_2 = 0.005$, although the random error of estimated altitude is smaller, estimation is not unbiased. Low-pass filter designed to extract high-frequency noise of pressure altitude performs better under this circumstance, but high-pass filter designed to extract low-frequency noise of altitude integrated by acceleration performs worse. Hence the estimated altitude is

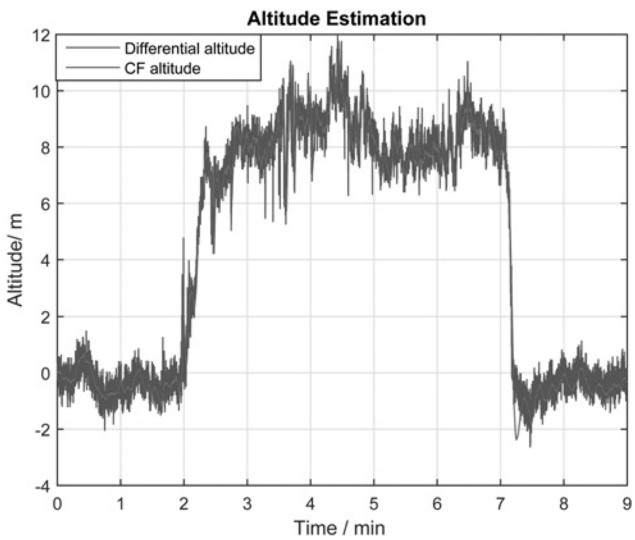


**Fig. 10** *Flight experiment by using differential altitude measurement and complementary filter*

**Fig. 11** *Unmanned quadrotor used in the flight experiment*

smoother. When $k_1 = 0.8$, $k_2 = 0.02$, the random error of the estimated altitude is greater, because low-pass filter designed to extract high-frequency noise performs worse on this condition. When $k_1 = 0.25$, $k_2 = 0.015$, both of the low-frequency random noise of altitude integrated by acceleration and high-frequency random noise of pressure altitude are small. It is because the coefficients balance the contribution of low-pass filter and high-pass filter better, hence the estimated altitude is optimal.

A flight experiment has been carried out to test the performance of the proposed scenario, and the performance of the experimental result as shown in Fig. 10. As shown in Fig. 11, the unmanned quadrotor is equipped with rover barometer, IMU system and other sensors. The raw sensor data is collected at a rate equal to 50 Hz. The unmanned quadrotor starts hovering at 2 min after taking off. The random noise of differential altitude is decreased by using complementary filter (Figs. 10 and 11).

## 6 Conclusion

In this paper, differential altitude measurement and complementary filter is combined together for altitude data fusion. Meanwhile, low-cost IMU and barometer are utilised in the experiments. This novel scenario has been tested by means of stair and flight test, and a considerable performance has been observed. On the one hand, the algorithm of complementary filter is more accurate and high-dynamic. On the other hand, the approach can suppress the altitude drift by using differential altitude measurement. Moreover, it can reduce the stochastic error of altitude estimation by adopted complementary filter algorithm. By adjusting the feedback coefficients, the result of the tests is encouraging.

## 7 Acknowledgment

This research has been supported by NSFC (National Natural Science Foundation of China) ‘Frequency tuning adaptive control method and experiment for the drive and sense modes of Silicon/MEMS gyroscope (61274117)’ in China.

## 8 References

1 Szafranski, G., Czyba, R., Janusz, W., *et al.*: ‘Altitude estimation for the UAV¡¯s applications based on sensors fusion algorithm’. 2013 Int. Conf. on Unmanned Aircraft Systems (ICUAS), Atlanta, GA, 2013, pp. 508–515

2 Yong, H., Ziyang, Z., Zhisheng, W.: ‘Federated filter based multi-sensor fault-tolerant altitude determination system for UAV’. 2008 Chinese Control and Decision Conf., Yantai, Shandong, 2008, pp. 2030–2034

3 Rao, M., Presti, L.L., Samson, J.: ‘Iterative altitude-aiding algorithm for improved GNSS positioning’, *IET Radar Sonar Navig.*, 2011, **5**, (7), pp. 788–795

4 Xiaoming, Z., Guobin, C., Jie, L., *et al.*: ‘Calibration of triaxial MEMS vector field measurement system’, *IET Sci. Meas. Technol.*, 2014, **8**, (6), pp. 601–609. 9p

5 Gasior, P., Gardecki, S., Gosliski, J., *et al.*: ‘Estimation of altitude and vertical velocity for multirotor aerial vehicle using Kalman Filter’, *Recent Adv. Autom. Robot. Meas. Tech. Adv. Intell. Syst. Comput.*, 2014, **267**, pp. 377–385

6 Kim, Y.-K., Choi, S.-H., Kim, H.-W., *et al.*: ‘Performance improve- ment and altitude estimation of pedestrian dead-reckoning system using a low-cost MEMS sensor’. 2012 12th Int. Conf. on Control, Automation and Systems (ICCAS), 17–21 October 2012, vol., no., pp. 1655–1660

7 Yanjun, L., Yang, L., Shenglin, Y.: ‘Research on the algorithm of information fusion for altitude of UAV’. 2013 Fourth Int. Conf. on Intelligent Systems Design and Engineering Applications, 6–7 November 2013, vol., no., pp. 523–526

8 Bevermeier, M., Walter, O., Peschke, S., *et al.*: ‘Barometric altitude estimation combined with map-matching in a loosely-coupled Kalman-filter’. 2010 Seventh Workshop on Positioning Navigation and Communication (WPNC), 11–12 March 2010, vol., no., pp. 128–134

9 Eynard, D., Vasseur, P., Demonceaux, C., *et al.*: ‘UAV altitude estimation by mixed stereoscopic vision’. 2010 IEEE/RSJ Int. Conf. on Intelligent Robots and Systems (IROS), Taipei, 2010, pp. 646–651

10 Cherian, A., Andersh, J., Morellas, V., *et al.*: ‘Autonomous al- titude estimation of a UAV using a single onboard camera’. IEEE/RSJ Int. Conf. on Intelligent Robots and Systems, 2009. IROS 2009. St. Louis, MO, 2009, pp. 3900–3905

11 Karunarathne, M.S., Ekanayake, S.W., Pathirana, P.N.: ‘An adaptive complementary filter for inertial sensor based data fusion to track upper body motion’. 2014 Seventh Int. Conf. on Information and Automation for Sustainability (ICIAfS), Colombo, 2014, pp. 1–5

12 Gui, P., Tang, L., Mukhopadhyay, S.: ‘MEMS based IMU for tilting measure- ment: Comparison of complementary and kalman filter based data fusion’. 2015 IEEE 10th Conf. on Industrial Electronics and Applications (ICIEA), Auckland, 2015, pp. 2004–2009

13 Tseng, S.P., Li, W.L., Sheng, C.Y., *et al.*: ‘Motion and attitude estimation using inertial measurements with complementary filter’. 2011 Eight Control Conf. (ASCC), Asian, Kaohsiung, 2011, pp. 863–868

14 Li, X., He, C., Wang, Y., *et al.*: ‘Generalized complementary filter for at- titude estimation based on vector observations and cross products’. 2015 IEEE Int. Conf. on Information and Automation, Lijiang, 2015, pp. 1733–1737

15 Savage, P.G.: ‘Strapdown analytics’ (Strapdown Associates, Inc., Maple Plain, Minnesota, 2000)

16 Parviainen, J., Kantola, J., Collin, J.: ‘Differential barometry in personal navigation’. 2008 IEEE/ION Position, Location and Navigation Symp., 5–8 May 2008, vol., no., pp. 148–152